

Synthesis of lamellar mesostructured calcium phosphates using *n*-alkylamines as structure-directing agents in alcohol/water mixed solvent systems

Nobuaki Ikawa^a · Yasunori Oumi^a · Tatsuo Kimura^b · Takuji Ikeda^c · Tsuneji Sano^{a,*}

^a *Department of Applied Chemistry, Graduate School of Engineering, Hiroshima University, Higashi-Hiroshima 739-8527, Japan*

^b *National Institute of Advanced Industrial Science and Technology (AIST), Shimoshidami, Moriyama-ku, Nagoya 463-8560, Japan*

^c *AIST, Tohoku, Nigatake, Miyagino-ku, Sendai 983-8551, Japan*

E-mail: tsano@hiroshima-u.ac.jp, Fax: +81-82-424-5494

Abstract

Lamellar mesostructured calcium phosphates constructed by ionic bonds were prepared by using *n*-alkylamines ($n\text{-C}_n\text{H}_{2n+1}\text{NH}_2$, $n = 8\text{--}18$) at room temperature in the mixed solvent systems of aliphatic alcohol ($\text{C}_n\text{H}_{2n+1}\text{OH}$, $n = 1\text{--}4$) and water, and the synthetic conditions were investigated in detail. The mixed solvent systems suppressed the formation of crystalline calcium phosphates like brushite ($\text{CaHPO}_4 \cdot 2\text{H}_2\text{O}$), monetite (CaHPO_4), and so on as discrete phases, successfully affording pure lamellar mesostructured calcium phosphates. Although the excess amount of water in the reaction systems allowed the formation of hydrated phases like brushite, the formation of brushite was suppressed by using the mixed solvent systems. Synthesis at low temperatures in the mixed solvent systems prevented calcium phosphate species from crystallizing to provide crystalline calcium phosphates like anhydrous monetite. Other crystalline phases such as hydroxyapatite ($\text{Ca}_{10}(\text{PO}_4)_6(\text{OH})_2$) were not also formed in the conditions with the Ca/P molar ratios in the range of 0.7–1.0 in the starting mixtures. The Ca/P molar ratio of the lamellar mesostructured calcium phosphates was ca. 1.0, calculated by ^{31}P MAS NMR and elemental analysis data. Interestingly, the kind of alcohols strongly influenced the solubilities of calcium phosphate species and *n*-alkylamines, and then lamellar mesostructured phases were obtained with some morphological variation.

Keywords: Calcium phosphate, Lamellar mesostructure, Alkylamine, Alcohol/water mixed solvent

Introduction

Calcium phosphate compounds with biocompatibility have been widely applied to biomaterials such as bone prosthesis and adsorbents for biomolecules [1-3]. Hydroxyapatite that is one of crystalline calcium phosphate compounds has actually used as artificial bone in practical clinic [4]. However, patients who need a medical treatment of their fractures with synthetic bones must bear his privation for a long time until the complete curing of the bone tissue because of the low physical strength between bionic and original bones [5]. Composites of inorganic calcium phosphate and organic collagen have drawn much attention as artificial bone and scaffold materials [6,7] because the presence of collagen promotes the crystallization of the calcium phosphate. Therefore, many research groups have investigated the potential applications of the inorganic-organic composite materials and their robust achievements have been already verified [8-10]. Such composite materials are applicable not only to bone prosthesis but also to a model system of inorganic-organic hybrid materials including precursors of porous materials prepared using some organic molecules and assemblies as structure directing agents.

The preparation of ordered mesoporous materials has been conducted by using amphiphilic organic molecules which are self-organized in aqueous solutions and their hydrophilic headgroups are interacted with soluble inorganic species [11-14]. The mesoporous materials have some specific features such as high surface area and high adsorption capacity including uniformity and periodicity of tunable mesopores [15-17], which are widely applicable to adsorbents and catalytic supports [18-21]. Crystalline calcium phosphates used as adsorbents have showed relatively low surface areas ($\sim 100 \text{ m}^2 \text{ g}^{-1}$) so far. The value is obviously inferior to those of surfactant-templated mesoporous materials [22-24]. Recently, bioactive mesoporous silica whose surfaces were covered with apatite layer grown in simulated body fluid was reported as a high capacity vessel for drug delivery and scaffold materials [25]. The paper also suggested the potential application of mesoporous calcium phosphate as biomaterials.

Synthetic procedures of ordered mesoporous materials have been advanced by some strategies to control mesostructures [26,27], compositions [28-32], and so on mainly through the investigation on silica-based materials. Inorganic-organic mesostructured composites act as precursors of ordered mesoporous materials formed through self-assembly of surfactant molecules attached with inorganic species and condensation of the inorganic species [15-17]. The surfactant-templating method has applied to the synthesis of other mesoporous solids, leading to the

successful preparation of a large number of mesoporous and mesostructured metal oxides and phosphates [28-46]. However, it is quite difficult to synthesize surfactant-templated mesoporous materials composed of pure calcium phosphates because the inorganic frameworks are connected through ionic bonds between Ca^{2+} and phosphate ions. Some research groups have commented only the possibility to form lamellar mesostructured calcium phosphates [47-52]. In general, it is recognized that calcium phosphate-based materials with ionic frameworks are more preferentially crystallized than other covalently bonded phosphate-based materials. Actually, in the previous reports on the synthesis of mesostructured calcium phosphates using surfactants, crystallization of calcium phosphate species could not be suppressed and then mesostructured precursors composed of calcium phosphates were not obtained except for lamellar phases. Even the formation of the lamellar phases is not proved by powerful analyses such as TEM so distinctly.

Recently, we found the successful synthetic procedure of a lamellar mesostructured calcium phosphate by using *n*-hexadecylamine in the ethanol/water mixed solvent system, which could suppress the crystallization of calcium phosphate species and control the solubility of calcium phosphate species [53]. In the present study, we investigated the effects of the synthetic conditions such as alcohol/water molar ratio, Ca/P molar ratio, reaction temperature, the kind of alcohol, and the alkyl chain length of *n*-alkylamine in more detail on the formation of the lamellar mesostructured calcium phosphate.

Experimental

Materials

All the *n*-alkylamines ($n\text{-C}_n\text{H}_{2n+1}\text{NH}_2$, $n = 8, 10, 12, 16, \text{ and } 18$) were obtained from Tokyo Kasei Kogyo Co. Phosphoric acid (85% H_3PO_4), aqueous solution of ammonia (25% NH_3), and calcium acetate monohydrate ($\text{Ca}(\text{OAc})_2 \cdot \text{H}_2\text{O}$) were obtained from Wako Chemical Co. Aliphatic alcohols such as methanol (MeOH), ethanol (EtOH), *n*-propanol (PrOH) and *n*-butanol (BuOH) were also purchased from Wako Chemical Co. and used without further purification. Calcium hydroxide ($\text{Ca}(\text{OH})_2$) was obtained from Kanto Chemical Co.

Synthesis of mesostructured calcium phosphate

Lamellar mesostructured calcium phosphate was prepared as follows. *n*-Alkylamine and 85% H_3PO_4 were added to a mixed solvent of alcohol and water. A white slurry mixture was obtained after stirring over 1 h. $\text{Ca}(\text{OAc})_2 \cdot \text{H}_2\text{O}$ and 25% NH_3 were added to the white slurry mixture under

vigorous stirring and the stirring was maintained for 15 min. The starting mixture ($\text{Ca}(\text{OAc})_2$: H_3PO_4 : $n\text{-C}_n\text{H}_{2n+1}\text{NH}_2$: 0.5NH_3 : $40n\text{-C}_n\text{H}_{2n+1}\text{OH}$: $40\text{H}_2\text{O}$) was statically kept for another 5 days at room temperature. The product was filtered, washed with EtOH repeatedly, and air-dried.

Characterization

X-ray diffraction (XRD) patterns were obtained by using a Rigaku RINT 2000 with graphite monochromatized Cu K α radiation (40 kV, 30 mA). The compositions were measured by inductively coupled plasma atomic emission spectroscopy (ICP-AES, Seiko SPS 7700).

Thermogravimetric (TG) analyses were conducted by using a Seiko TG/DTA320 thermal analyser.

Transmission electron microscopic (TEM) images were taken by a JEOL JEM-2010 microscope, operated at 200 kV. ^{31}P MAS NMR spectra were obtained by using a Bruker DRX-400 spectrometer with a 7 mm zirconia rotor at a resonance frequency of 161.9 MHz with a spinning rate of 6 kHz. The spectra were accumulated with 4.5 μs pulses and 40 s recycle delay. 85%

H_3PO_4 aqueous solution was used as a chemical shift reference. ^{13}C CP/MAS NMR spectra were also collected by using the same spectrometer at 100.7 MHz with a spinning rate of 4 kHz, 6.8 μs pulses, and 15 s recycle delay. Tetramethylsilane was used as a chemical shift reference. Scanning electron microscopic (SEM) images were taken by a JEOL JSM-6320FS to observe morphology of the products.

Results and discussion

The crystallization of calcium phosphate formed through rapid reaction between Ca^{2+} and phosphate ions is dramatically fast than other inorganic compounds constructed by covalent bond. Indeed, there are few reports on the preparation of amorphous calcium phosphate before its transformation into more stable crystalline phases [54]. Since interaction between surfactant molecules and phosphate ions is lost by the formation of discrete crystalline calcium phosphates, it is necessary to control mesostructures of calcium phosphates before rapid formation of crystalline calcium phosphates. Accordingly, we suggest a two-step reaction. Alkylammonium phosphates are utilized as intermediates [55] and reacted with calcium sources under conditions that keep ionic bonds between alkylammonium and phosphate ions during generation of mesostructured calcium phosphates.

Effect of EtOH/H $_2$ O molar ratio

The synthesis of lamellar mesostructured calcium phosphate was carried out by using $n\text{-C}_{16}\text{H}_{33}\text{NH}_2$ in the mixed solvent of ethanol (EtOH) and water. The starting mixtures were prepared by mixing 85% H_3PO_4 , $\text{Ca}(\text{OAc})_2 \cdot \text{H}_2\text{O}$, and 25% NH_3 in the mixed solvent with the different molar ratios of EtOH and water. The composition of the starting mixtures was presented as $\text{Ca}(\text{OAc})_2 : \text{H}_3\text{PO}_4 : n\text{-C}_{16}\text{H}_{33}\text{NH}_2 : 0.5\text{NH}_3 : 80(\text{EtOH}+\text{H}_2\text{O})$. The XRD patterns of the products prepared in the presence and absence of $n\text{-C}_{16}\text{H}_{33}\text{NH}_2$ are shown in Fig. 1. Even when the synthesis was conducted in the presence of $n\text{-C}_{16}\text{H}_{33}\text{NH}_2$, a hydrated product such as brushite ($\text{CaHPO}_4 \cdot 2\text{H}_2\text{O}$) was mainly observed in the aqueous system (Fig. 1(A)(a)) [56]. Brushite was also obtained in the absence of the surfactant in the aqueous system (Fig. 1(B)(a)). With the increase in the amount of EtOH in the reaction systems containing $n\text{-C}_{16}\text{H}_{33}\text{NH}_2$, the peaks due to brushite disappeared (Fig. 1(A)(b)-(d)), indicating that the formation of brushite is suppressed in the EtOH/ H_2O systems. The synthesis of crystalline calcium phosphates in the EtOH/ H_2O systems without surfactant was already reported and the preferential formation of brushite is suppressed by using EtOH as a co-solvent [57]. Therefore, similar synthesis was also conducted in the absence of the surfactant. Peaks due to brushite disappeared gradually by increasing the amount of EtOH in the reaction systems without $n\text{-C}_{16}\text{H}_{33}\text{NH}_2$ (Fig. 1(B)(a)-(d)). Peaks due to monetite (CaHPO_4) that is one of anhydrous calcium phosphate phases appeared by increasing the amount of EtOH (Fig. 1(B)(c)-(e)). In contrast, a peak with the d -spacing of 4.5 nm and the higher order diffractions that are possibly assignable to lamellar phases appeared in low diffraction angles of the reaction systems with $n\text{-C}_{16}\text{H}_{33}\text{NH}_2$ (Fig. 1(A)(b)-(d)). The formation of lamellar mesostructured calcium phosphate was confirmed further by TEM observation, showing clear striped patterns (Fig. 2). The results reveal that the lamellar mesostructured calcium phosphate can be obtained in the mixed solvent systems [53]. It is considered that further increase of the amount of EtOH was not useful for the reaction between $\text{Ca}(\text{OAc})_2$ and H_3PO_4 because $\text{Ca}(\text{OAc})_2 \cdot \text{H}_2\text{O}$ could not be dissolved in the mixtures (Fig. 1(A)(e) and (B)(e)). Accordingly, only lamellar hexadecylammonium phosphate [$(n\text{-C}_{16}\text{H}_{33}\text{NH}_3^+)(\text{H}_2\text{PO}_4^-)$] was formed in the ethanolic system containing $n\text{-C}_{16}\text{H}_{33}\text{NH}_2$ (Fig. 1(A)(e)).

Effect of Ca/P molar ratio

Lamellar mesostructured calcium phosphates were synthesized under the conditions with different Ca/P molar ratios in the starting mixtures. The composition of the starting mixture was

0.7–1.5Ca(OAc)₂ : H₃PO₄ : *n*-C₁₆H₃₃NH₂ : 0.5NH₃ : 80(EtOH+H₂O). The EtOH/H₂O molar ratio was simultaneously changed with the variation in the Ca/P molar ratio under the condition with the fixed H₂O/Ca molar ratio (40) in the reaction system. The XRD patterns of the products obtained at the Ca/P molar ratios of 0.7–1.5 in the starting mixtures are shown in Fig. 3. In the products obtained at the Ca/P molar ratios ranging from 0.7 to 1.0, the peaks observed at $2\theta = 1.5\text{--}6.0^\circ$ are corresponded to the formation of lamellar mesostructured calcium phosphate ($d_{001} = 4.5$ nm) (Fig. 3(A)(a)-(c)). Several peaks, which are not assignable to crystalline calcium phosphates, were also observed in high diffraction angles (Fig. 3(B)(a)-(c)). Some of the peaks are considered to be due to the ordering in the calcium phosphate framework of the lamellar phase. However the assignment of these peaks has not been achieved yet because of the broadening of the peaks due to distortion of the layered structure. With the further increase in the Ca/P molar ratio from 1.2 to 1.5, the peaks at $2\theta = 15\text{--}25^\circ$ (Fig. 3(B)(d)-(e)) as well as the peaks assignable to the lamellar mesostructured calcium phosphate disappeared (Fig. 3(A)(d)-(e)) although small broad peaks assignable to initial crystalline hydroxyapatite phase appeared at $2\theta = 26$ and 32° (Fig. 3(B)(d)-(e)) [54, 58]. The result indicates that the formation of the lamellar mesostructured calcium phosphate occurred at the Ca/P molar ratios from 0.7 to 1.0 because the hydroxyapatite phase was formed preferentially at higher Ca/P molar ratios than 1.0. Hydroxyapatite (Ca₁₀(PO₄)₆(OH)₂) known as anhydrate crystalline calcium phosphate was formed in the non-aqueous solvent system under the calcium-rich conditions. When the composition of the starting mixture was changed into 0.7Ca(OAc)₂ : H₃PO₄ : *n*-C₁₆H₃₃NH₂ : 0.5NH₃ : 40EtOH : 40H₂O, however, lamellar mesostructured calcium phosphate was obtained with the slight formation of brushite. The result would be caused by the H₂O-rich condition (H₂O/Ca molar ratio of 40/0.7) because the presence of H₂O in the reaction system is necessary for controlling the dissolution of the calcium source.

The ³¹P MAS NMR measurements were applied to get further information on the calcium phosphate frameworks and the spectra of the products prepared by changing the Ca/P molar ratios in the range of 0.7–1.5 in the starting mixtures are shown in Fig. 4. In the ³¹P MAS NMR spectrum of the product obtained at Ca/P = 0.7, three peaks were observed at 2.1, 0.4, and –1.7 ppm (Fig. 4(b)). In compared with the spectrum of (*n*-C₁₆H₃₃NH₃⁺)(H₂PO₄[–]) (Fig. 4(a)), the small peak at 0.4 ppm is considered to be assigned to P atoms in the similar salt. With the increase in the Ca/P molar ratio, the intensity of the shoulder peak at around –1.7 ppm decreased gradually while that of the peak at 2.1 ppm was enhanced (Fig. 4(b)-(e)). The ³¹P MAS NMR spectra were also measured

with ^1H - ^{31}P cross-polarization (CP) technique (not shown here). The intensity of the peak at 2.1 ppm was not enhanced in the ^{31}P CP/MAS NMR spectrum, being consistent with the lack of protons neighboring to P atoms in the calcium phosphate framework. However, the CP enhancement was observed for the product obtained at $\text{Ca/P} = 0.9$, revealing the presence of two PO_4 units, probably, $[\text{PO}_4]^{3-}$ and $[\text{HPO}_4]^{2-}$ or $[\text{H}_2\text{PO}_4]^-$, are present in the framework of the lamellar mesostructured calcium phosphate [59, 60].

Effect of the reaction temperature

The synthesis was also conducted at different temperatures under the condition with the composition of $\text{Ca}(\text{OAc})_2 : \text{H}_3\text{PO}_4 : n\text{-C}_{16}\text{H}_{33}\text{NH}_2 : 0.5\text{NH}_3 : 40\text{EtOH} : 40\text{H}_2\text{O}$. After the starting mixture was stirred for 15 min, the mixture was aged at room temperature, 50 or 70 °C statically. The XRD patterns of the products prepared at room temperature, 50 and 70 °C are shown in Fig. 5. Although all of the XRD patterns showed the formation of lamellar mesostructured calcium phosphates, the d_{001} values (4.0 nm) of the lamellar phases obtained by heating at 50 and 70 °C were smaller than that of the lamellar phase (4.5 nm) at room temperature (Fig. 5(a)-(c)). In addition, the products obtained by heating contained monetite and the amount of that was increased by elevating the synthetic temperature [61]. None of typical striped patterns characteristic for lamellar mesostructured materials were found in the TEM images of the products obtained at 50 and 70 °C. Additional experiment was carried out to get more information about this phase. After each product (0.5 g) was stirred at 60 °C for 5 h in EtOH (150 g), filtered, and washed with EtOH at 60 °C, only the peaks in the low diffraction angles disappeared completely. It is reasonable to be considered that this phase would not be lamellar but organic, probably a moiety of *n*-hexadecylamine and/or $(n\text{-C}_{16}\text{H}_{33}\text{NH}_3^+)(\text{H}_2\text{PO}_4^-)$. The crystallization of monetite would occur more preferentially than that of the lamellar mesostructured calcium phosphate at higher temperatures. The result exhibits that the control of the reaction temperature enables to suppress the crystallization of monetite under the condition, being strongly useful for the mesostructural control of calcium phosphates.

The synthetic regions that several calcium phosphates could be obtained under synthetic conditions with various EtOH/H₂O and Ca/P molar ratios at r.t. are schematized in Fig. 6. In the region of higher Ca/P molar ratio than 1.0, the predominant formation of hydroxyapatite occurred in the mixed solvent system regardless of the EtOH/H₂O molar ratio. When the Ca/P molar ratio

was lower than 1.0, brushite was formed in the H₂O-rich system. The reaction between (*n*-C₁₆H₃₃NH₃⁺)(H₂PO₄⁻) and calcium source did not occur in pure EtOH system. At higher aging temperature than r.t., monetite was formed. In the synthetic region that the formations of crystalline calcium phosphates were suppressed by the control of synthetic conditions, the lamellar mesostructured calcium phosphate could be formed. This result strongly indicates that the interaction between hexadecylammonium and phosphate ions must be maintained to obtain the lamellar mesostructured calcium phosphate during the reaction of Ca²⁺ ions and hexadecylammonium phosphate (Fig. 7).

Effect of alcohol as co-solvent

Effect of co-solvents was investigated by using a series of aliphatic alcohols. The composition of the starting mixture was Ca(OAc)₂ : H₃PO₄ : *n*-C₁₆H₃₃NH₂ : 0.5NH₃ : 80(ROH+H₂O), R = CH₃, C₂H₅, C₃H₇, and C₄H₉. The ROH/H₂O molar ratio was changed from 0/100 to 96/4. The mixture of lamellar mesostructured calcium phosphate and brushite was obtained at the MeOH/H₂O molar ratio of 25/75. The formation of brushite was suppressed with an increase in the amount of MeOH, leading to the successful preparation of pure lamellar phase in the range of MeOH/H₂O molar ratio from 40/60 to 75/25. In the cases of the PrOH/H₂O and BuOH/H₂O systems, pure lamellar mesostructured calcium phosphate could be obtained at ROH/H₂O of 75/25. Under the conditions in the range of ROH/H₂O molar ratio from 50/50 to 25/75, only brushite was formed in both of the systems. The formation of brushite was also suppressed by increasing the amount of MeOH, PrOH and BuOH as well as EtOH. However, there is a difference in the range of the ROH/H₂O molar ratio to afford lamellar mesostructured calcium phosphate. The results are schematically summarized in Fig. 8. Lamellar phases were formed under restricted ROH/H₂O molar ratios in the reaction systems using aliphatic alcohols having longer alkyl chains. Actually, the range of the EtOH/H₂O molar ratio affording pure lamellar mesostructured calcium phosphate was narrower than that of the MeOH/H₂O molar ratio. As ROH with longer alkyl chains is not mixed with H₂O because hydrophobicity of the alcohol becomes strong, the reaction system seems to be relatively analogous to aqueous systems, which has a tendency to provide hydrated crystalline calcium phosphate phase such as brushite. Therefore, the effective range of the ROH/H₂O molar ratio becomes narrow with an increase in the alkyl chain length of alcohol, which prevents from the formation of lamellar mesostructured calcium phosphate. The results indicate that the kind of

alcohol is also important for controlling the solubility of the calcium source and the preferential formation of crystalline calcium phosphate phases.

The TEM images of the mesostructured calcium phosphates obtained by using a series of ROH in the mixed solvent systems with ROH/H₂O of 75/25 and 50/50 are shown in Fig. 9. Stripe patterns were clearly observed for all the products obtained at ROH/H₂O of 75/25 (Fig. 9(a), (d)-(f)). However, in addition to the stripe patterns (Fig. 9(b)), disordered stripe patterns were slightly observed for the product obtained at MeOH/H₂O of 50/50 (Fig. 9(c)). The SEM observation of the products was also conducted and the images of the products obtained at ROH/H₂O of 75/25 are shown in Fig. 10. Morphologies of the lamellar mesostructured calcium phosphates were plate-like and the size increased gradually by using ROH with longer alkyl chains, revealing that the particle size of the lamellar phases is controllable in the mixed solvent systems according to the alkyl chain length of alcohol.

Possible structure of lamellar mesostructured calcium phosphate

On the basis of the ³¹P MAS NMR results, it is considered that the framework structure of the lamellar mesostructured calcium phosphate contains two phosphate units. The elemental analysis showed that Ca/P molar ratios in the frameworks were almost consistent with those in the corresponding starting mixtures. Thermogravimetric curve of the lamellar mesostructured compound with the Ca/P molar ratio of 1.0 is shown in Fig. 11. Main mass losses of 23.0 and 28.7 mass % were observed below 200 °C and between 200 and 600 °C, which correspond to dehydration and combustion of organic moiety, respectively. After the lamellar phase was calcinated at 600 °C for 10 h, a white solid was obtained. The XRD peaks of the white solid were assigned to a calcium pyrophosphate (Ca₂P₂O₇) (Fig. 12). On the basis of the mass loss below 600 °C, the formula could be presented as (C₁₆H₃₃NH₃⁺)_{0.6}Ca²⁺(HPO₄²⁻)_{0.4}(PO₄³⁻)_{0.6}.

Lamellar mesostructured calcium phosphates were prepared by using *n*-alkylamines with different alkyl chain lengths as structure-directing agents. Calcium hydroxide was used as a calcium source instead of calcium acetate monohydrate, because the products containing both of lamellar mesostructured calcium phosphate (main product) and alkylammonium phosphate salt (by-product) were obtained by using *n*-C_{*n*}H_{2*n*+1}NH₂ except for using *n*-C₁₆H₃₃NH₂ when calcium acetate monohydrate was used. The XRD patterns of the products obtained from a series of starting mixtures with Ca(OH)₂ : H₃PO₄ : *n*-C_{*n*}H_{2*n*+1}NH₂ (*n* = 8–18) : 40EtOH : 40H₂O are shown

in Fig. 13. The patterns contained the peaks due to both unreacted calcium hydroxide and lamellar mesostructured calcium phosphate. The d_{001} values corresponding to the lamellar phases were changed in the range of 2.8–4.8 nm (2.8 nm for $n = 8$, 3.4 nm for $n = 10$, 3.7 nm for $n = 12$, 4.5 nm for $n = 16$, and 4.8 nm for $n = 18$). Conformation of the alkyl chains of the surfactant molecules (*n*-hexadecylamine) in the lamellar mesostructured calcium phosphate was investigated by ^{13}C CP/MAS NMR. The ^{13}C CP/MAS NMR spectrum of the lamellar mesostructured calcium phosphate obtained from the starting mixture with the composition of $\text{Ca}(\text{OAc})_2 : \text{H}_3\text{PO}_4 : n\text{-C}_{16}\text{H}_{33}\text{NH}_2 : 0.5\text{NH}_3 : 40\text{EtOH} : 40\text{H}_2\text{O}$ are shown in Fig. 14. Several peaks due to carbon atoms in *n*-hexadecylamine were observed and the peak at 32 ppm can be assigned to carbon atoms in all-*trans* methylene ($-\text{CH}_2-$) chains [62, 63]. Fig. 15 shows the relation between the d_{001} spacing and the number of carbon atoms in the alkyl chains of the *n*-alkylamines. In accordance with the correlation, a slope of the straight line was calculated to be 0.185 nm/ CH_2 . Since the distance between two adjacent carbon atoms are expressed as 0.127 nm/ CH_2 in an all-*trans* alkyl chains [64], the alkyl chains are arranged in the lamellar phases as double layers with a tilt angle of ca. 46° . Also, the wall thickness of the mesostructured calcium phosphates was estimated to be ca. 1.2 nm.

Conclusions

Lamellar mesostructured calcium phosphates constructed through ionic bonds were successfully synthesized by using *n*-alkylamines as structure-directing agents under a wide variety of conditions. Morphology of lamellar mesostructured calcium phosphates was also controlled by changing the alkyl chain length of alcohol used as co-solvents. It was mainly important for synthesis of the lamellar mesostructured calcium phosphates to control both solubility of calcium source and crystallization of calcium phosphate species. The controlled synthesis is possible in the mixed solvent systems of alcohols and water that allows the interaction between the surfactant molecules and calcium phosphate species and the suppression of the discrete crystallization of calcium phosphate species. These materials are promising as biomaterials such as bone prosthesis and adsorbents for biomolecules, and the crystallization and solubility controlled synthesis will open the new route to obtain mesostructured materials whose frameworks are constructed by ionic bonds.

References

1. Jarcho M (1981) *Clin Orthop Relat Res* 157:259
2. Ducheyne P, Qiu Q (1999) *Biomaterials* 20:2287
3. Kim H W, Georgiou G, Knowles J C, Koh Y H, Kim H E (2004) *Biomaterials* 25:4203
4. Hulbert S F, Young F A, Mathews R S, Klawitter J J, Talbert C D, Stelling F H (1970) *J Biomed Mater Res* 4:433
5. De Groot K, De Putter C, Smitt P, Driessen A (1981) *Sci Ceram* 11:433
6. Hartgerink J D, Beniash E, Stupp S I (2001) *Science* 294:1684
7. Kikuchi M, Itoh S, Ichinose S, Shinomiya K, Tanaka J (2001) *Biomaterials* 22:1705
8. Cölfen H, Mann S (2003) *Angew Chem, Int Ed* 42:2350
9. Silva G A, Czeisler C, Niece K L, Beniash E, Harrington D A, Kessler J A, Stupp S I (2004) *Science* 27:1352
10. Elemans J A A W, Rowan A E, Nolte R J M (2003) *J Mater Chem* 13:2661
11. Yanagisawa T, Shimizu T, Kuroda K, Kato C (1990) *Bull Chem Soc Jpn* 63:988
12. Inagaki S, Fukushima Y, Kudoda K (1993) *J Chem Soc, Chem Commun* 680
13. Kresge C T, Leonowicz M E, Roth W J, Vartuli J C, Beck J S (1992) *Nature* 359:710
14. Beck S, Vartuli J C, Roth W J, Leonowicz M E, Kresge C T, Schmitt K D, C T-W Chu, Olson D H, Sheppard E W, McCullen S B, Higgins J B, Schlenker J L (1992) *J Am Chem Soc* 114:10834
15. Zhao D, Feng L, Huo Q, Melosh N, Fredrickson G H, Chmelka B F, Stucky G D (1998) *Science* 279:548
16. Zhao X S, Lu G Q, Millar G J (1996) *Ind Eng Chem Res* 35:2075
17. Selvam P, Bhatia S K, Sonwane C G (2001) *Ind Eng Chem Res* 40:3237
18. Sayari A (1996) *Chem Mater* 8:1840
19. Corma A (1997) *Chem Rev* 97:2373
20. Taguchi A, Schüth F (2005) *Micropor Mesopor Mater* 77:1
21. Schüth F (2003) *Angew Chem, Int Ed* 42:3604
22. Monma H (1995) *Inorg Mater* 2:401
23. Rodriguez-Lorenzo L M, Vallet-Regí M (2000) *Chem Mater* 12:2460
24. Uota M, Arakawa H, Kitamura N, Yoshimura T, Tanaka J, Kijima T (2005) *Langmuir* 21:4724
25. Vallet-Regí M, Ruiz-González L, Izquierdo-Barba I, González-Calbet J M (2006) *J Mater Chem* 16:26
26. Huo Q, Leon R, Petroff P M, Stucky G D (1995) *Science* 268:1324
27. Huo Q, Margolese D I, Stucky G D (1996) *Chem Mater* 8:1147
28. Behrens P (1996) *Angew Chem, Int Ed* 35:515
29. Sayari A, Liu P (1997) *Micropor Mater* 12:149
30. Schüth F (2001) *Chem Mater* 13:3184
31. Tiemann M, Fröba M (2001) *Chem Mater* 13:3211
32. Kimura T (2005) *Micropor Mesopor Mater* 77:97
33. Yu C, Tian B, Zhao D (2003) *Curr Opin Solid State Mater Sci* 7:191

34. Gao Q, Xu R, Chen J, Li R, Li S, Qui S, Yue Y J (1997) *Chem Mater* 9:457
35. Kimura T, Sugawara Y, Kuroda K (1999) *Chem Mater* 11:508
36. Mal N K, Fujiwara M, Ichikawa S, Kuraoka K (2002) *J Ceram Soc Jpn* 110:890
37. Mal N K, Ichikawa S, Fujiwara M (2003) *Chem Commun* 872
38. Roca M, Haskouri J E, Cabrera S, Beltrán-Porter A, Alamo J, Beltrán-Porter D, Macros M D, Amorós P (1998) *Chem Commun* 1883
39. Dasgupta S, Agarwal M, Datta A (2002) *J Mater Chem* 12:162
40. Jiménez-Jiménez J, Maireles-Torres P, Olivera-Pastor P, Rodríguez-Castellón E, Jiménez-López A, Jones D J, Rozière J (1998) *Adv Mater* 10:812
41. Jones D J, Aptel G, Brandhorst M, Jacquín M, Jiménez-Jiménez J, Jiménez-López A, Maireles-Torres P, Piwonski I, Rodríguez-Castellón E, Zajac J, Rozière J (2000) *J Mater Chem* 10:1957
42. Bhaumik A, Inagaki S (2001) *J Am Chem Soc* 123:691
43. Guo X, Ding W, Wang X, Yan Q (2001) *Chem Commun* 709
44. Chang J-S, Park S-E, Gao Q, Férey G, Cheetham A K (2001) *Chem Commun* 859
45. Tarafdar A, Biswas S, Pramanik N K, Pramanik P (2006) *Micropor Mesopor Mater* 89:204
46. Mal N K, Ichikawa S, Fujiwara M (2002) *Chem Commun* 112
47. Ozin G A, Varaksa N, Coombs N, Davies J E, Perovic D D, Ziliox M (1997) *J Mater Chem* 7:1601
48. Soten I, Ozin G A (1999) *J Mater Chem* 9:703
49. Yao J, Tjandra W, Chen Y Z, Tam K C, Ma J, Soh B (2003) *J Mater Chem* 13:3053
50. Schmidt S M, McDonald J, Pineda E T, Verwilst A M, Chen Y, Josephs R, Ostefin A E (2006) *Micropor Mesopor Mater* 94:330
51. Tokuoka Y, Ito Y, Kitahara K, Niikura Y, Ochiai A, Kawashima N (2006) *Chem Lett* 35:1220
52. Zhao Y F, Ma J (2005) *Micropor Mesopor Mater* 87:110
53. Ikawa N, Oumi Y, Kimura T, Ikeda T, Sano T (2006) *Chem Lett* 35:948
54. Eanes E D, Gillissen I H, Posner A S (1965) *Nature* 208:365
55. Oliver S R J, Ozin G A (1998) *J Mater Chem* 8:1081
56. Sivakumar G R, Girija E K, Karukura S N, Subramanian C (1998) *Cryst Res Technol* 33:197
57. Larson M J, Thorsen A, Jensen S J (1985) *Calcif Tissue Int* 37:189
58. Kim S, Ryu H S, Shin H, Jung H S, Hong K S (2005) *Mater Chem Phys* 91:500
59. Aue W P, Roufosse A H, Glimcher M J, Griffin R G (1984) *Biochemistry* 23:6110
60. Miquel J L, Facchini L, Legrand A P, Rey C, Lemaitre J (1990) *Colloids Surfaces* 45:427
61. Furuichi K, Oaki Y, Imai H (2006) *Chem Mater* 18:229
62. Simonutti R, Comotti A, Bracco S, Sozzani P (2001) *Chem Mater* 13:771
63. Kooli F, Mianhui L, Alshahateet S F, Chen F, Yinghuai Z (2006) *J Phys Chem Solids* 67:926
64. Kitaigorodskii A I (1973) *Molecular Crystals and Molecules*, Academic Press, New York

Figure captions

Fig. 1 XRD patterns of the products obtained (A) with and (B) without $C_{16}H_{33}NH_2$. EtOH/H₂O ratio: (a) 0/100, (b) 25/75, (c) 50/50, (d) 75/25 and (e) 96/4.

Fig. 2 TEM image of lamellar mesostructured calcium phosphate obtained with EtOH/H₂O (50/50).

Fig. 3 XRD patterns at (A) low and (B) high angles of the products obtained at various Ca/P ratios: (a) 0.7, (b) 0.9, (c) 1.0, (d) 1.2 and (e) 1.5.

Fig. 4 ³¹P MAS NMR spectra of lamellar mesostructured calcium phosphates obtained at different Ca/P ratios: (a) $[C_{16}H_{33}NH_3^+][H_2PO_4^-]$, (b) 0.7, (c) 0.9, (d) 1.0 and (e) 1.2.

Fig. 5 XRD patterns of the products prepared at (a) room temperature, (b) 50 and (c) 70 °C.

Fig. 6 The synthetic region of lamellar mesostructured calcium phosphates at room temperature.

Fig. 7 Proposed formation route of lamellar mesostructured calcium phosphate.

Fig. 8 Effect of aliphatic alcohol on synthesis of lamellar mesostructured calcium phosphate with *n*- $C_{16}H_{33}NH_2$.

Fig. 9 TEM images of lamellar mesostructured calcium phosphates obtained in the ROH/H₂O systems. (a) MeOH/H₂O (75/25), (b) and (c) MeOH/H₂O (50/50), (d) EtOH /H₂O (75/25), (e) PrOH /H₂O (75/25) and (f) BuOH /H₂O (75/25).

Fig. 10 SEM images of lamellar mesostructured calcium phosphates obtained in the ROH/H₂O (75/25) systems: (a) MeOH, (b) EtOH, (c) PrOH and (d) BuOH.

Fig. 11 Thermogravimetric curve of lamellar mesostructured calcium phosphate with Ca/P molar ratio of 1.0.

Fig. 12 XRD pattern of the calcined product of lamellar mesostructured calcium phosphate with the Ca/P molar ratio of 1.0 at 600 °C.

Fig. 13 XRD patterns of lamellar mesostructured calcium phosphates prepared using (a) $n\text{-C}_8\text{H}_{17}\text{NH}_2$, (b) $n\text{-C}_{10}\text{H}_{21}\text{NH}_2$, (c) $n\text{-C}_{12}\text{H}_{25}\text{NH}_2$, (d) $n\text{-C}_{16}\text{H}_{33}\text{NH}_2$ and (e) $n\text{-C}_{18}\text{H}_{37}\text{NH}_2$.

Fig. 14 ^{13}C CP/MAS NMR spectrum of lamellar mesostructured calcium phosphate obtained from the starting mixture of $\text{Ca}(\text{OAc})_2 : \text{H}_3\text{PO}_4 : n\text{-C}_{16}\text{H}_{33}\text{NH}_2 : 0.5\text{NH}_3 : 40\text{EtOH} : 40\text{H}_2\text{O}$.

Fig. 15 Relationship between d -spacing and carbon number in the alkyl chain of n -alkylamine.

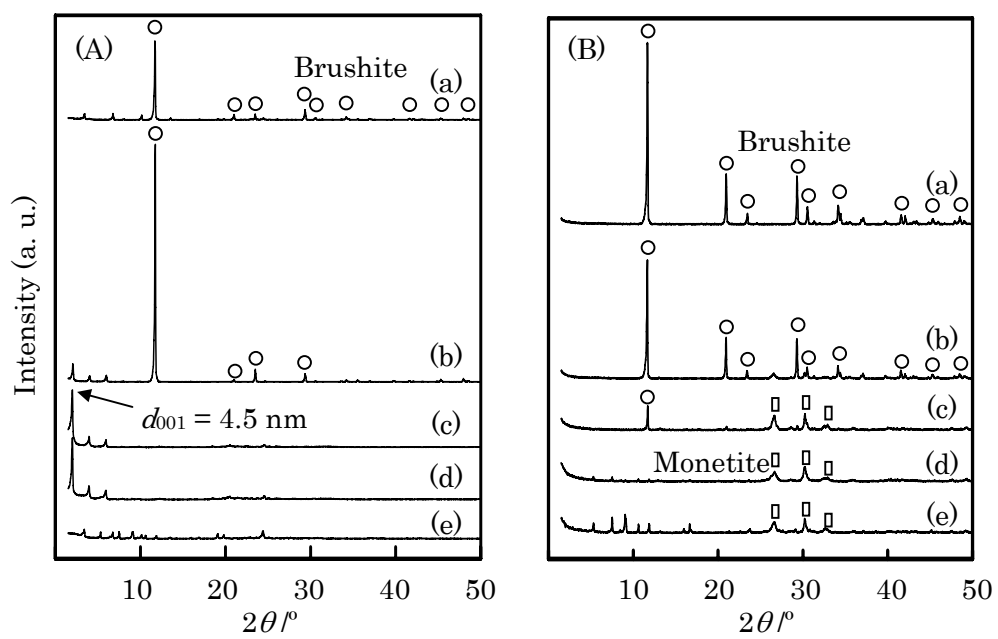


Fig. 1

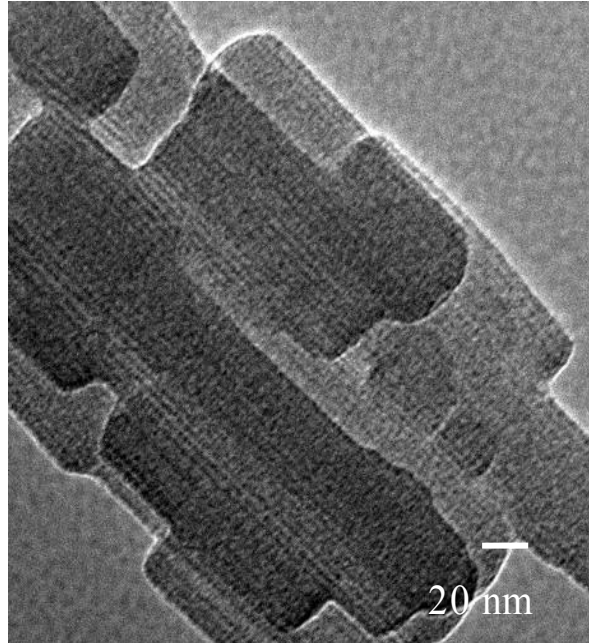


Fig. 2

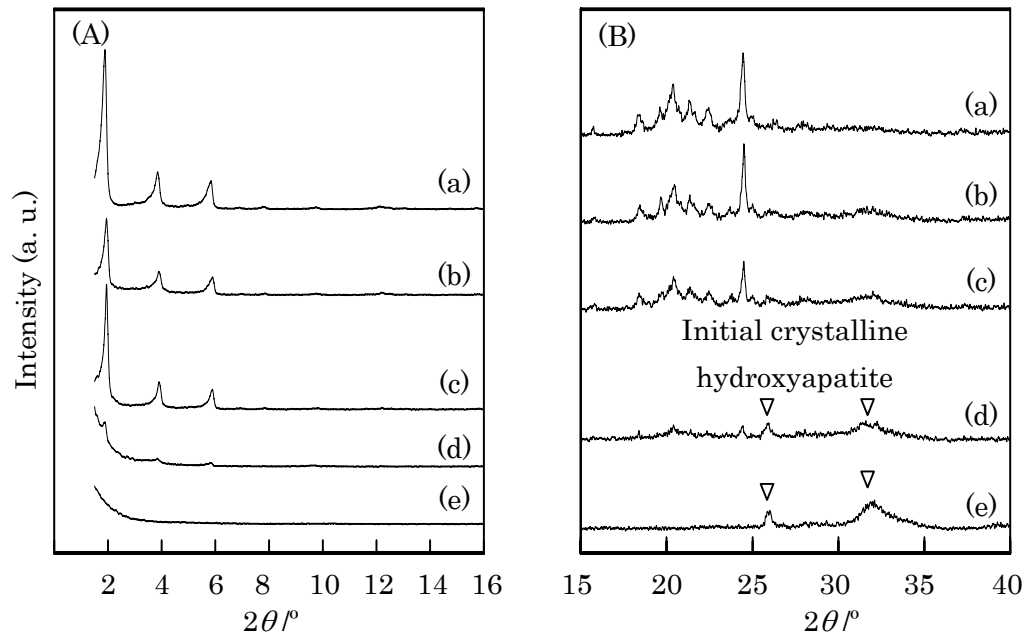


Fig. 3

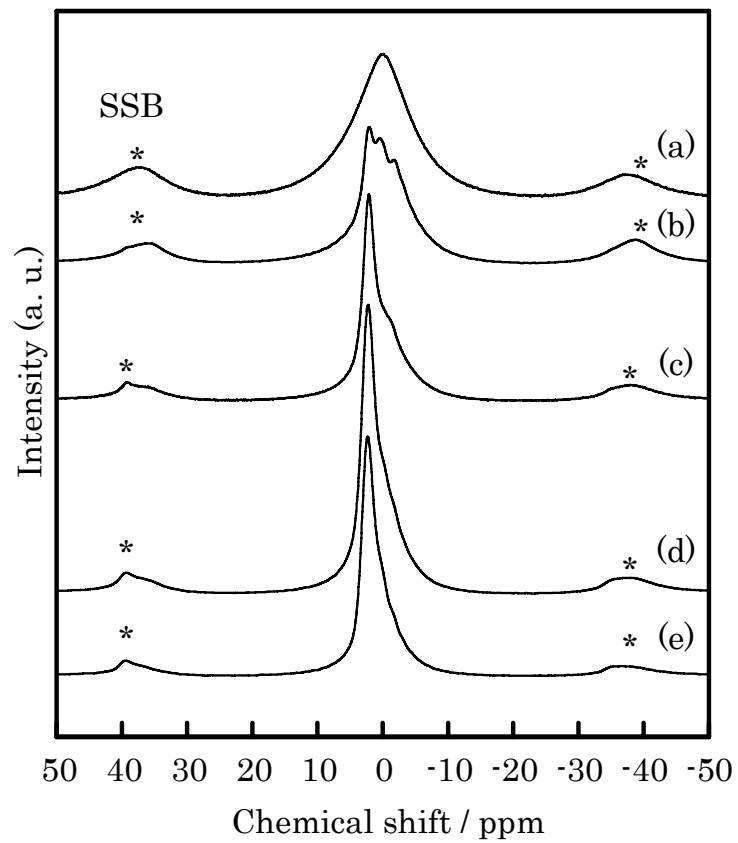


Fig. 4

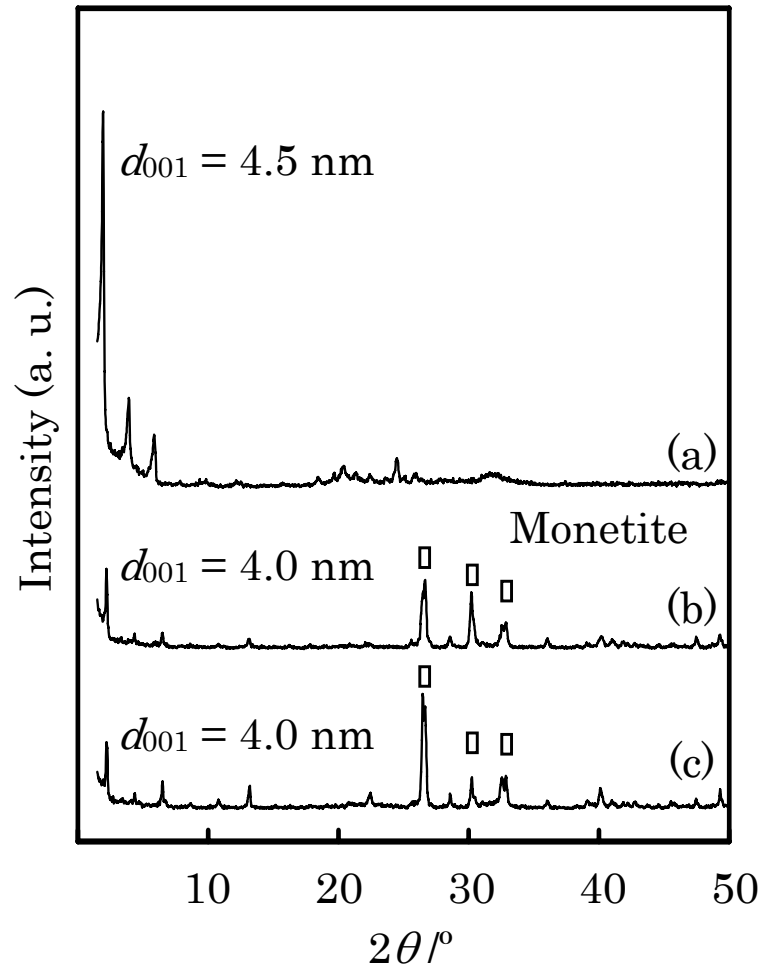


Fig. 5

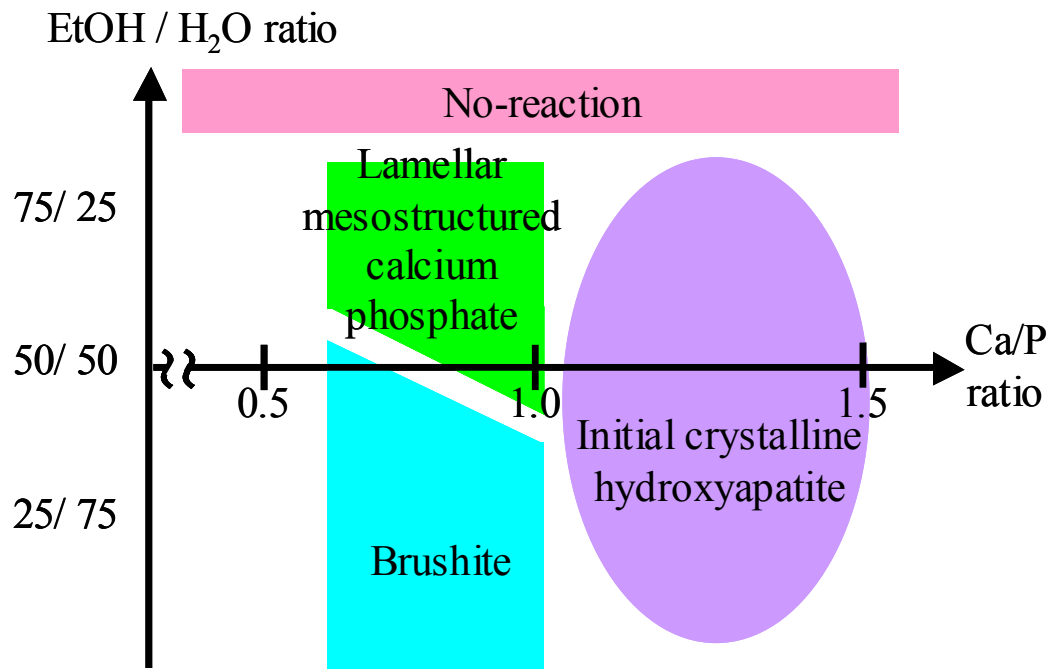


Fig. 6

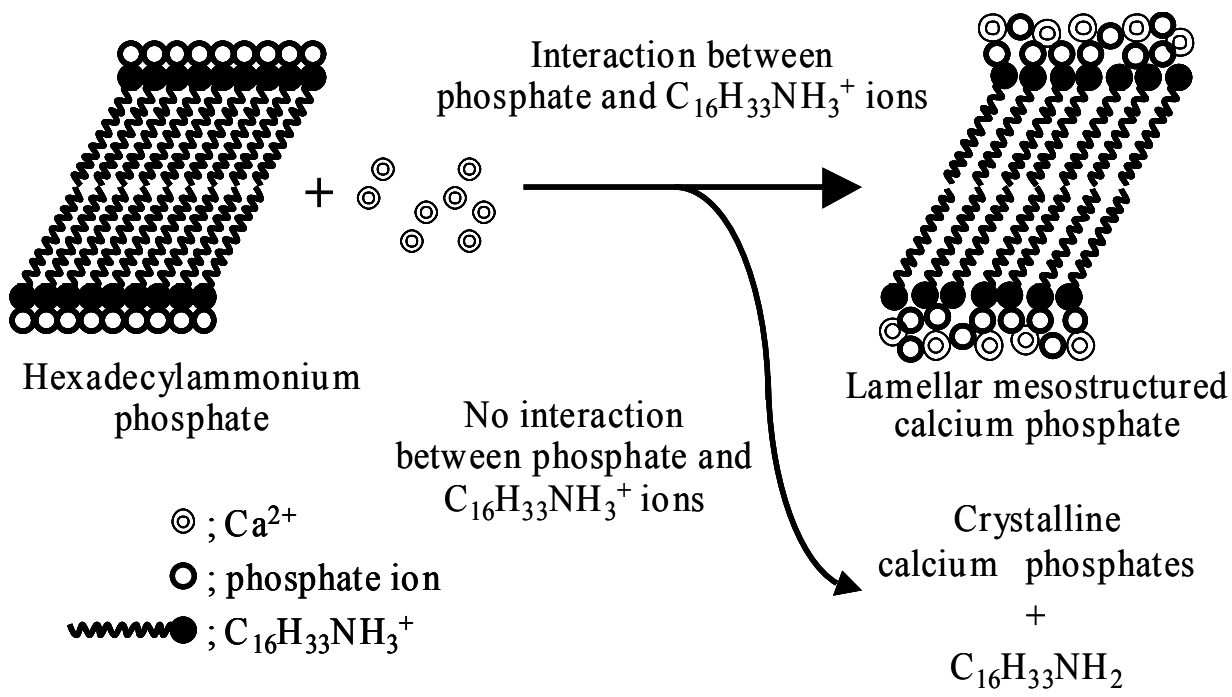


Fig. 7

ROH/H₂O ratio

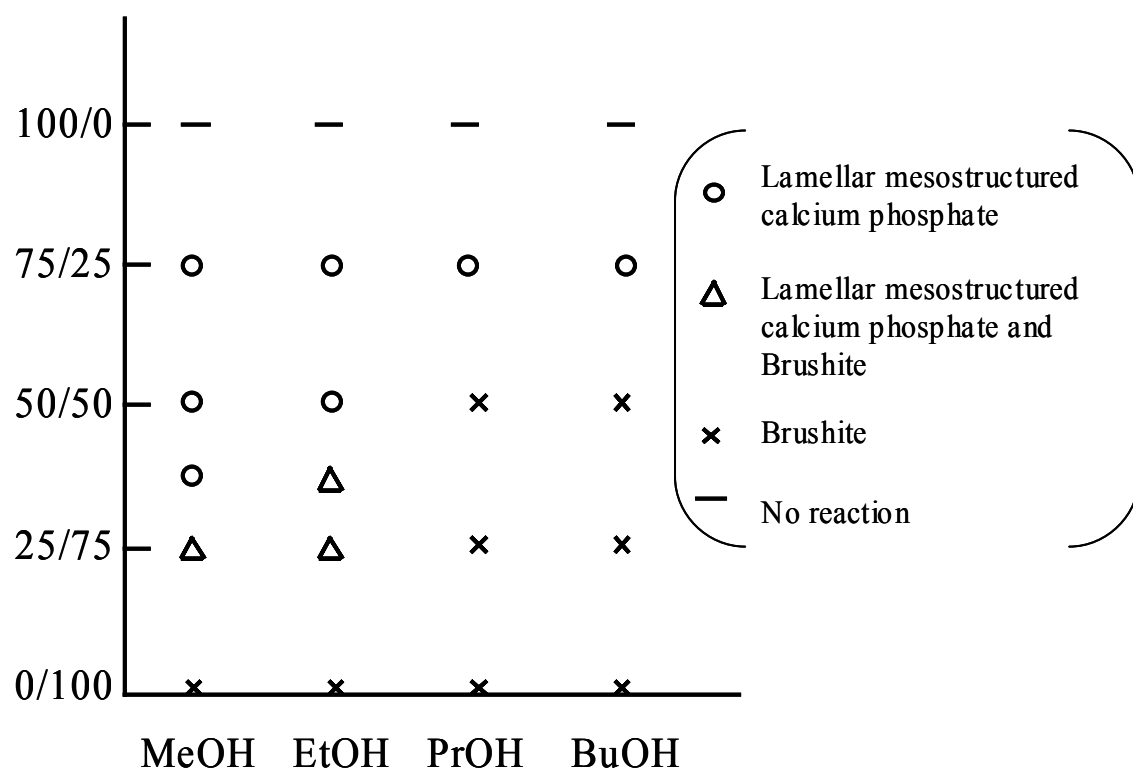


Fig. 8

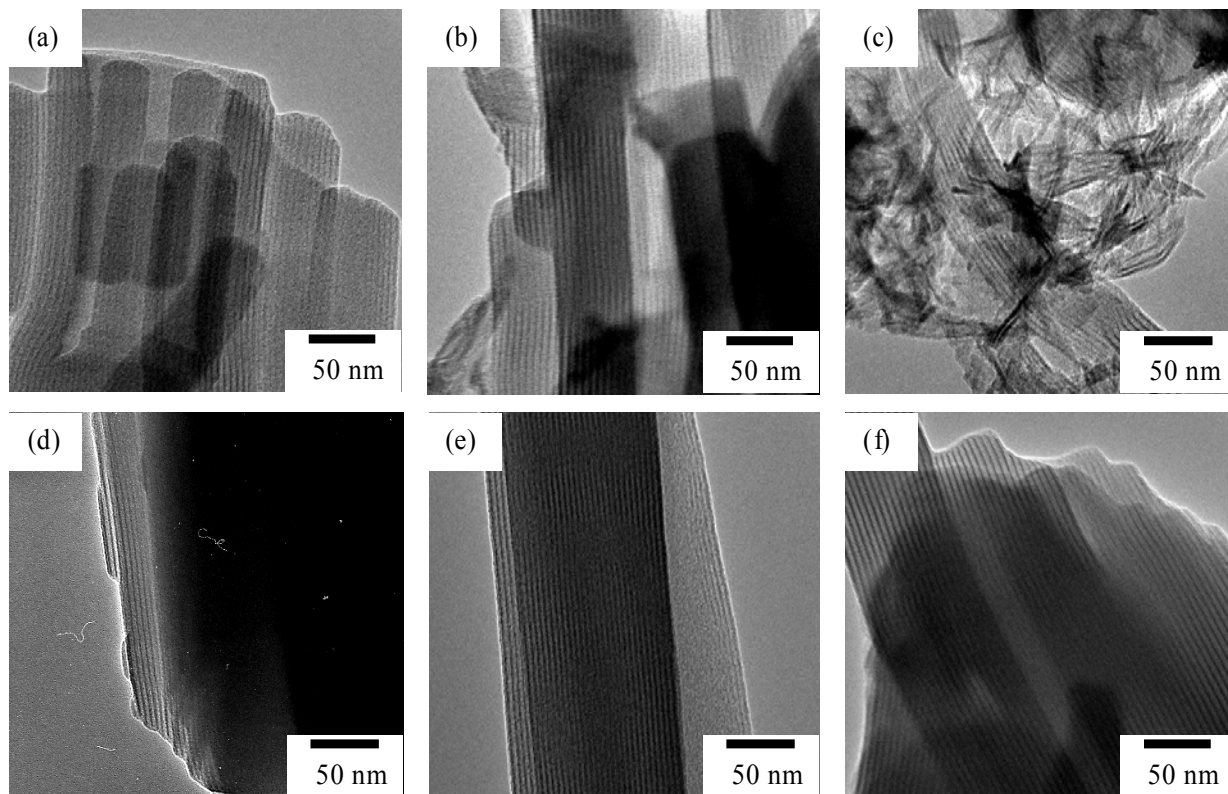


Fig. 9

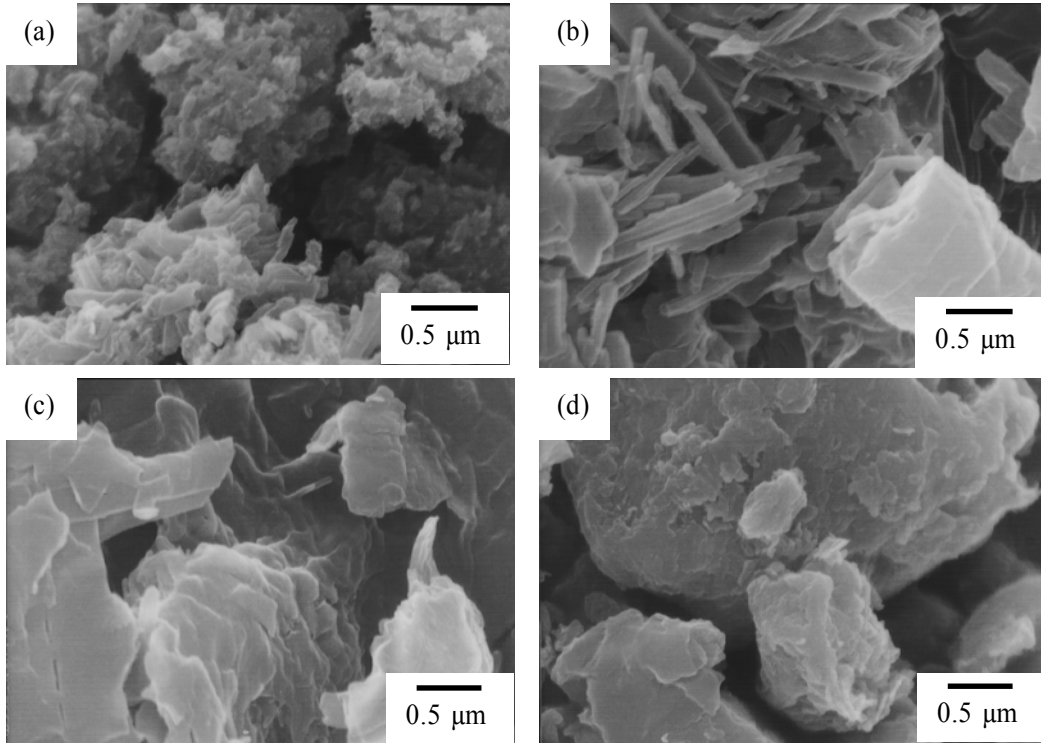


Fig. 10

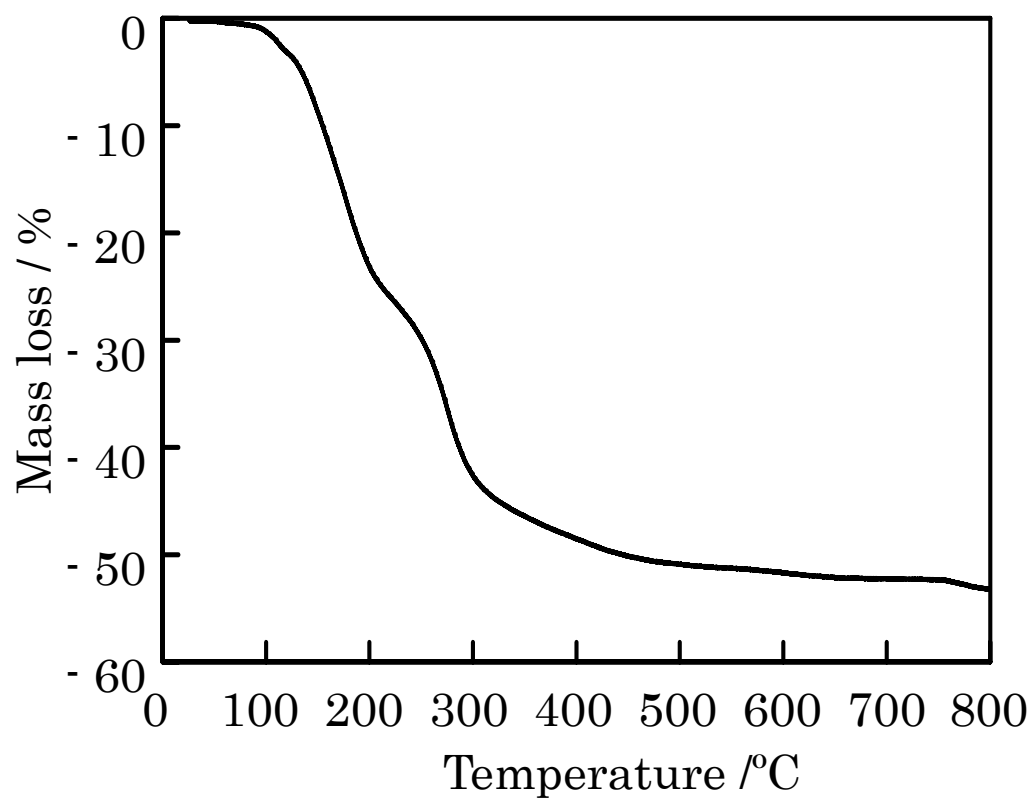


Fig. 11

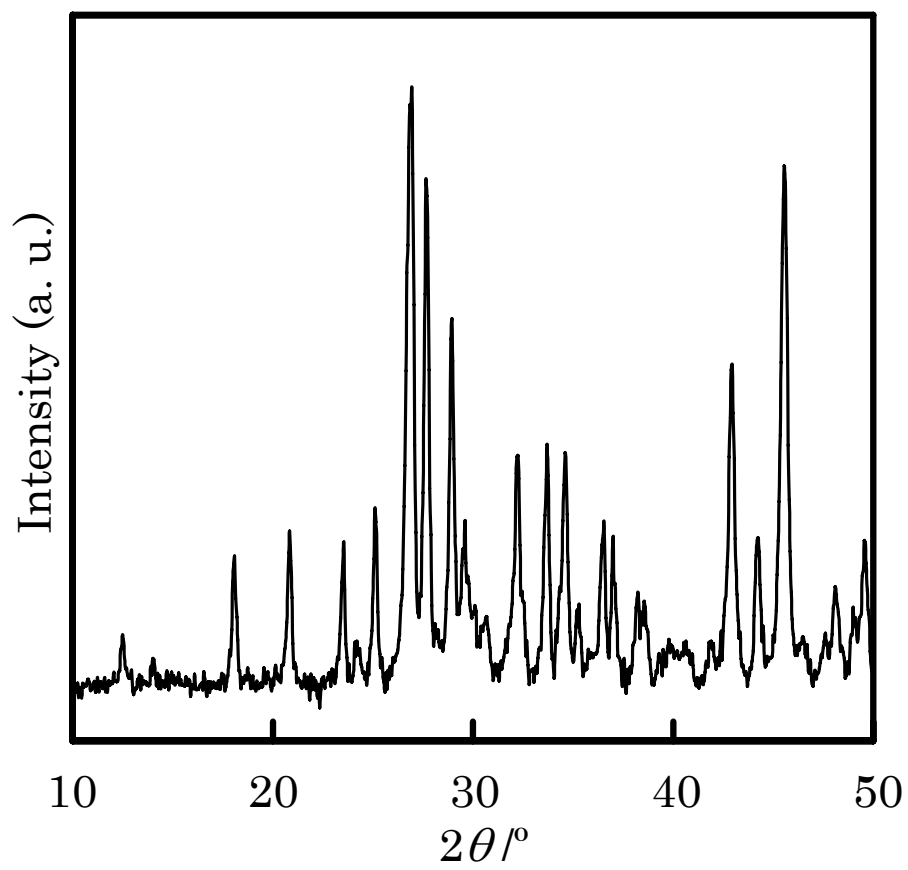


Fig. 12

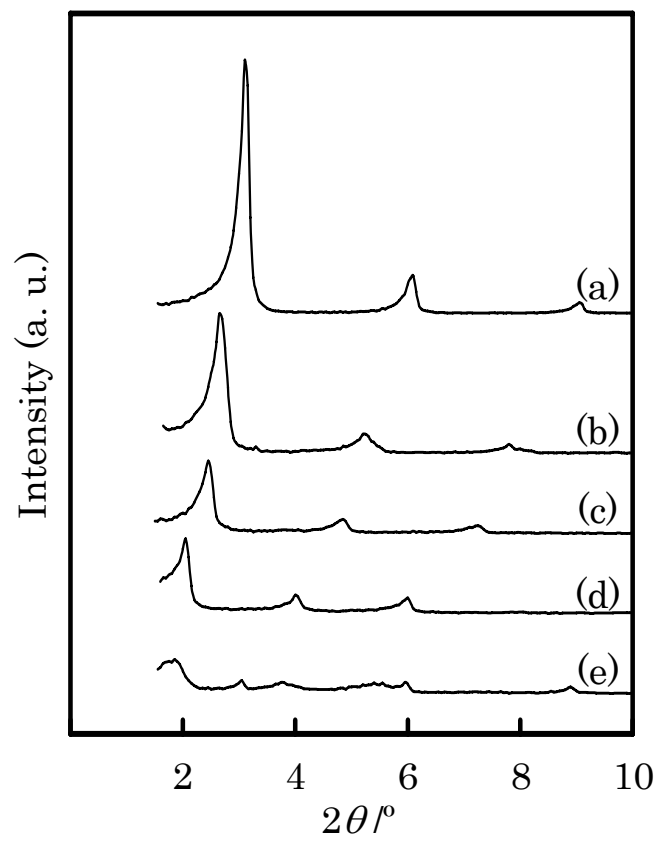


Fig. 13

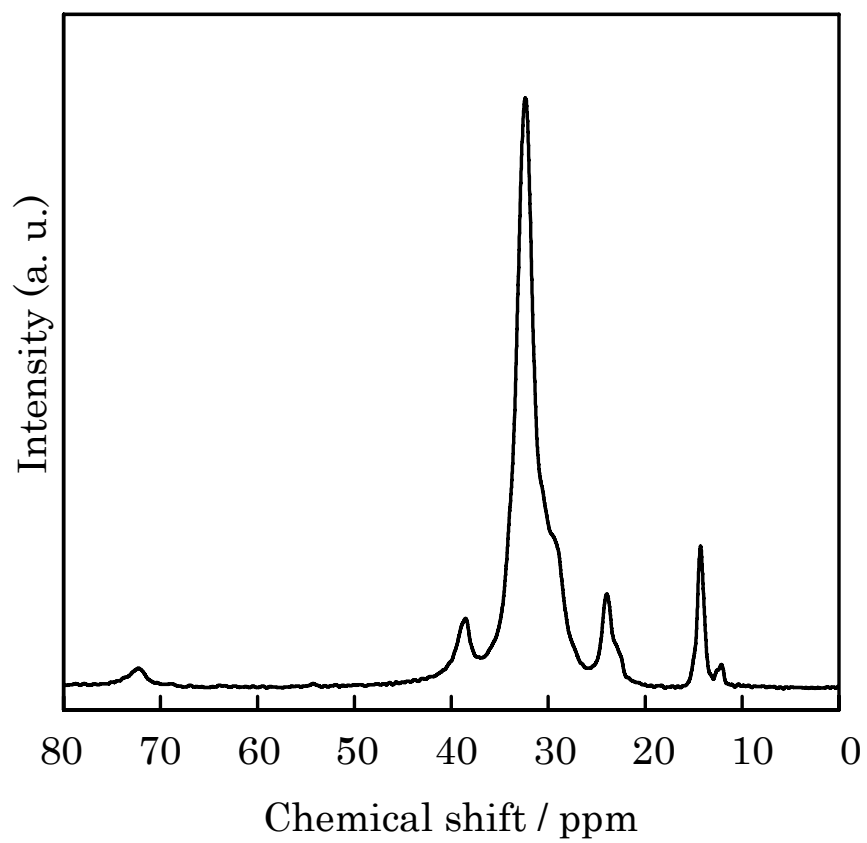


Fig. 14

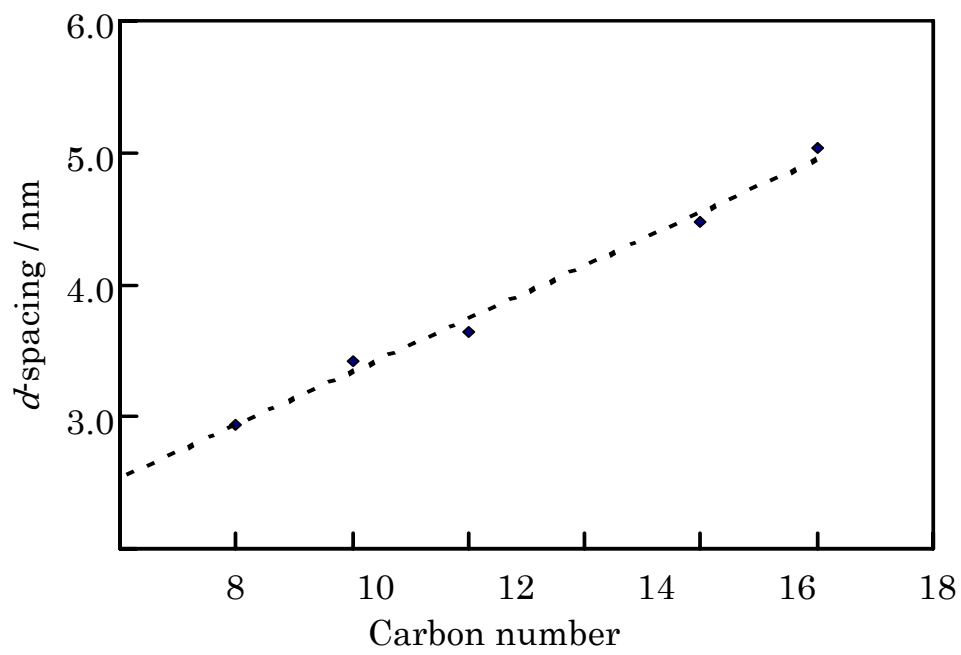


Fig. 15